The role of functionalization on the colloidal stability of aqueous fullerene C60 dispersions prepared with fullerides

João Paulo V. Damasceno, Ferdinand Hof, Olivier Chauvet, Aldo J.G. Zarbin, A. Pénicaud

▶ **To cite this version:**

João Paulo V. Damasceno, Ferdinand Hof, Olivier Chauvet, Aldo J.G. Zarbin, A. Pénicaud. The role of functionalization on the colloidal stability of aqueous fullerene C60 dispersions prepared with fullerides. Carbon, 2021, 173, pp.1041-1047. 10.1016/j.carbon.2020.11.082 . hal-03194268

HAL Id: hal-03194268
https://hal.science/hal-03194268

Submitted on 9 Apr 2021

HAL is a multi-disciplinary open access archive for the deposit and dissemination of scientific research documents, whether they are published or not. The documents may come from teaching and research institutions in France or abroad, or from public or private research centers.

L'archive ouverte pluridisciplinaire **HAL**, est destinée au dépôt et à la diffusion de documents scientifiques de niveau recherche, publiés ou non, émanant des établissements d'enseignement et de recherche français ou étrangers, des laboratoires publics ou privés.

The Role of Functionalization on the Colloidal Stability of Aqueous Fullerene C_{60} Dispersions Prepared with Fullerides

João Paulo V. Damasceno,[a,b] Ferdinand Hof,[b] Olivier Chauvet,[c] Aldo José G. Zarbin,[,a] and Alain Pénicaud[*,b]*

[a]Department of Chemistry, Federal University of Paraná (UFPR), Centro Politécnico, 81531-980, Curitiba, Paraná, Brazil.

[b]Centre de Recherche Paul Pascal, CRPP UMR5031-CNRS / Université de Bordeaux, 115 Avenue du Dr Albert Schweitzer, 33600 Pessac France.

[c]Institut des Materiaux Jean Rouxel, IMN, Univesity de Nantes, CNRS, France.

*Corresponding Author. Tel: +55 41 33613176. Email: aldozarbin@ufpr.br (Aldo José G. Zarbin)

*Corresponding Author. Tel. +33 5 56843028. Email: alain.penicaud@crpp.cnrs.fr (Alain Pénicaud)

ABSTRACT

Aqueous dispersions of fullerene C_{60} were prepared from fulleride solutions in tetrahydrofuran, followed by air oxidation, transfer to water and solvent evaporation. Fulleride exposition to air produces charged fullerene dispersions in THF that can be transferred to water to produce aqueous fullerene dispersions, stable for months.

KEYWORDS

Fullerene C_{60}; Fulleride solutions; Aqueous dispersions; Colloidal stability; Electrostatic stabilization.

1. INTRODUCTION

Fullerenes, and more precisely buckminsterfullerene C_{60} as its most well-known representative, are molecular carbon allotropes.[1,2] C_{60} and other fullerenes can be solubilized as molecular species in different solvents,[3] like toluene, benzene, and CS_2 and concentrations up to 50 g L^{-1} can be reached in naphthalene based solvents.[3–5] In contrast, C_{60} is less soluble in chlorinated or polar solvents such as tetrahydrofuran (THF), acetonitrile, dimethyl sulfoxide (DMSO) and almost insoluble in methanol or water.

There are different approaches to enhance the solubility of fullerenes.[3] The most common is to functionalize C_{60} with groups chosen to enhance the solubility in targeted solvents.[3,6] A well-known example is [6,6]-phenyl-C_{60}-butyric acid methyl ester (PCBM), a functionalized C_{60} derivative, ubiquitous in organic solar cells, soluble in aromatic and chlorinated solvents.[7] Water solubility can also be achieved by covalently grafting hydroxyl groups[3,8–10] generating fullerenols, which are dispersible in water as nanoparticles[8,11–14] or soluble as individual molecular species with high functionalization degree as in $C_{60}(OH)_{36\text{-}44}$[15], which have been exploited in biological studies.[8,11–14] Another method to increase the solubility in polar solvents is based on the reduction of C_{60}.[6,16–18] Solutions containing reduced fullerenes, commonly called fulleride solutions, are usually prepared by three methods: *(i)* reaction between the carbon material and alkaline or alkaline-earth metals by melting or in vapour phase, *(ii)* reductive dissolution using those metals in ammonia or in naphthalene solutions, *(iii)* electrochemical methods in organic media.

A radically different approach to stabilize fullerene in aqueous media is by generating aqueous dispersions, typically stable for months, which contain polydisperse fullerene nanoparticles, up to 200 nm in size.[19–23] These dispersions can be prepared by solvent exchange methods,[22–24] sonication in solvent mixtures[11,19–21], methods based on dialysis,[25] or using fulleride solutions as precursors. Xu and collaborators[17] reported a

procedure to generate C_{60}^- anions and used them to prepare an aqueous dispersion by adding a THF solution of C_{60}^- into water, since naturally present oxygen in water causes C_{60}^- oxidation and aggregation.[17,26] In a more recent work, Wabra *et al*.[6] described the preparation of KC_{60} and K_2C_{60} and studied their reactivity with different molecules and water, and they claimed that C_{60}^{2-} reacts with water and produces a yellow solution of C_{60}^- that is stable for few weeks under inert conditions. However, C_{60}^- solutions in oxygen-free water should be red and not yellow. A yellowish colour is typically observed for dispersions of fullerenes.[19–23]

Herein, we report *(i)* the re-examination of the oxidation step of fulleride solutions that leads to the generation of metastable dispersions in THF, *(ii)* the transfer to water, producing, aqueous dispersions of C_{60}, in analogy to aqueous dispersions of graphene[27,28] and carbon nanotubes,[29,30] *(iii)* that these dispersions are stable regardless of the presence or not of functionalized fullerenes (*e.g.* fullerenols).

The generated aqueous dispersions exhibit concentrations up to 200 mg L^{-1}, mean particle sizes between 25 and 70 nm and zeta potentials from -10 to -50 mV depending on the precursor used and on the specific ratio between fulleride solution and water. The degree of C_{60} functionalization is higher when higher charged fullerenes (K_6C_{60}) are used in the dissolution step. Thus, at lower charge ratios (KC_{60}), metastable dispersions can be prepared that barely have any content of functionalized derivatives, and are not re-dispersible in water once dried due to their lyophobic nature. In contrast, dispersions exhibiting higher content of functionalized fullerenes can be dried and re-dispersed, evidencing the coexistence of C_{60} nanoparticles and fullerenols, which dramatically alters the physicochemical properties of fullerenes. Moreover, a sample of fullerenol containing no nanoparticles has been isolated and exhibits about 15 functional groups in average and is barely water soluble as expected for this low number of hydroxyl functions. These observations highlight the complexity and the

coexistence of water based aqueous dispersions of C_{60} and fullerenol solutions and the need for discriminating between the effects of these different chemical species.

This work demonstrates a pathway to produce in large quantities, concentrated aqueous dispersions of C_{60} composed by small nanoparticles. Additionally, it forms a basis for further studies to understand the electronic band structure and the nature of electrical charges in analogous dispersed systems such as carbon nanotubes and graphene. Furthermore, this study demonstrates that functionalized fullerenes and dispersed fullerenes can co-exist and urges caution for explaining specific phenomena or observed behaviour of those or related systems in biological, medical, and material science applications by considering either solely fullerenols or only dispersed fullerenes.

2. EXPERIMENTAL SECTION

2.1 Materials and chemicals

Fullerene C_{60} was acquired from Merck (>99.998 %), metallic potassium (98 %), toluene (≥ 99.8 %) and tetrahydrofuran (THF) from Sigma-Aldrich (≥ 99.8 %, HLPC, non-stabilized). Deuterated toluene was acquired from Sigma-Aldrich (99% deuterated) and deuterated water from Sigma-Aldrich (99.9 % deuterated). THF was purified by a Pure Solv 400-4-MD solvent purification system (Inert Corporation) that is attached directly to the glove box (Model: S1-DL, Inert Corporation), equipped with an oxygen purifier and H_2O and O_2 sensors. The as purified THF was distilled over NaK alloy prior to use inside the glove box. Typical O_2 concentrations during manipulation inside the glove box are ~0.4 ppm O_2/H_2O. Water was deionized in a Millipore equipment, model Elix 10, and the resistivity was equal to 18.2 MΩ. Stirring plates were acquired from Velp Scientifica, model MST Magnetic Stirrer.

2.2 Safety remark

The possible user of the reported synthesis protocol is reminded of the specific hazards related to the use of potassium metal. Safety precautions are advised for storage, handling and waste treatment. Potassium metal is extremely dangerous in contact with water or moisture, releasing hydrogen with enough heat to cause ignition or explosion. Peroxide formation may occur in containers that have been opened and remained in storage. May produce corrosive solutions on contact with water.

2.3 Synthesis of KC_{60} (1a) and K_6C_{60} (2a)

Preparation and dissolution of fullerene salts were performed in a glove box filled with argon (5 mbar above atmospheric pressure). KC_{60} and K_6C_{60} were prepared by molten potassium intercalation based on procedures from literature on nanotubes[31] and graphite.[28] Briefly, in a 2 mL glass vial, 8.8 mg (0.23 mmol) of cleaned metallic potassium (free of oxide layer) and 162.2 mg (0.23 mmol) of fullerene C_{60} were mixed for KC_{60} and 29.7 mg (0.76 mmol) of potassium and 91.2 mg (0.13 mmol) of C_{60} for K_6C_{60}. The solid mixture was heated on a hot plate at 180 °C and stirred with a stainless-steel spatula for 5 min until melting of the potassium was observed. Afterwards, the solid was heated for 55 min more minutes at 180 °C and stirred each 10 to 15 min. Afterwards, the sample was cooled to room temperature to yield the respective salt KC_{60} (**1a,** see Figure 1) and K_6C_{60} (**2a**).

2.4 Dissolution of KC_{60} (1b) and K_6C_{60} (2b), oxidation and preparation of aqueous dispersion

For all dissolutions, absolute THF (see preparation above) was used. The dissolution was carried out by placing 4 mg of KC_{60} or K_6C_{60} in a 21 mL glass vial and adding 20 mL of absolute THF. Subsequently, the mixture was shaken by hand and kept for about 15 min

inside the glove box, and was additionally shaken by hand each few minute. Both salts are soluble in THF and spontaneously produce fulleride solutions, KC_{60} as a dark red solution and K_6C_{60} as a light orange one. The supernatant was isolated in each case, yielding fulleride solution (**1b**) from KC_{60} and (**2b**) from K_6C_{60}.

2.5 Oxidation of the fulleride solution and preparation of the respective dispersion (1c; 2c)

The solutions (**1b**) and (**2b**) were removed from the glovebox, the vials opened at ambient atmosphere and air was bubbled four times with a 1.5 cc glass Pasteur pipette through the solution to promote oxidation of fulleride solutions. A color change was visible from dark red (**1b**) or light orange (**2b**) to brown (**1c**) or light gray (**2c**)**.** Both dispersions (**1c**) and (**2c**) were isolated and were stable for at least two months, without solvent evaporation and stored in contact with minimum amount of air as possible (no free volume inside the glass flask).

2.6 Preparation of the aqueous dispersions (1d; 2d)

Aqueous dispersions were prepared by mixing the dispersions (**1c**) and (**2c**) with deionized water in different mass proportions. 20 mL glass vial was filled with a weighted amount of deionized water and the vial was placed on a balance. Afterwards, the respective dispersion, directly after the oxidation step, was added by means of a glass Pasteur pipette. Then, the vial was kept in a hood for 2 days to allow THF evaporation. Aqueous dispersions of (**1d**) and (**2d**) were obtained having mass ratios of 1:8, 1:4, 1:2 or 1:1 respectively by combining 2.00, 3.75, 6.00 or 8.00 g of the respective oxidized fulleride solution (**1c**, or **2c**) with 16.00, 15.00, 12.00 or 8.00 g of water to achieve the above mentioned mass proportions.

The generated aqueous dispersions (**1d; 2d**) are slight to dark orange and are stable for at least 6 months.

3. RESULTS AND DISCUSSION

The aqueous dispersions of C_{60} reported here, (see Figure 1, details in Experimental Section and in ESI), were prepared starting from reduced fullerenes, (**1a** and **2a,** stoichiometry KC_{60} and K_6C_{60} respectively) which can be directly dissolved in polar solvents such as tetrahydrofuran (THF) (solutions **1b** and **2b**). By oxidation of the solutions (**1b**, **2b**) with air, the total charge in both systems is significant lowered, which causes aggregation within the samples, leading to the formation of dispersions of C_{60} nanoparticles in THF (**1c**, **2c**). These dispersions in THF can be added to water, and, after evaporation of THF, aqueous dispersions containing C_{60} nanoparticles are obtained that are stable for months (**1d**, **2d**). The initial amount of charge in **2a** is much higher than in **1a**, and is lowered significantly by the oxidation step and simultaneous production of significant amount of fullerenols (**3**) by side reactions.

The formation of KC_{60} and K_6C_{60} by the direct mixing of molten potassium and fullerene has been performed in analogy to the synthesis of reduced carbon nanotubes and intercalated graphite[28,31] and the resulting salts have been studied by XRD patterns (see Fig. S1, ESI) and Raman spectroscopy (see Fig. S2). The data suggest that the salts are predominantly KC_{60} and K_6C_{60} with minor contamination of C_{60} in the latter case.[2,32–35] Upon addition of THF to the C_{60} salts (**1a**, **2a**), a spontaneous dissolution can be observed that produces dark red (**1b**) or light orange (**2b**) fullerenide solutions in minutes without the need for stirring.

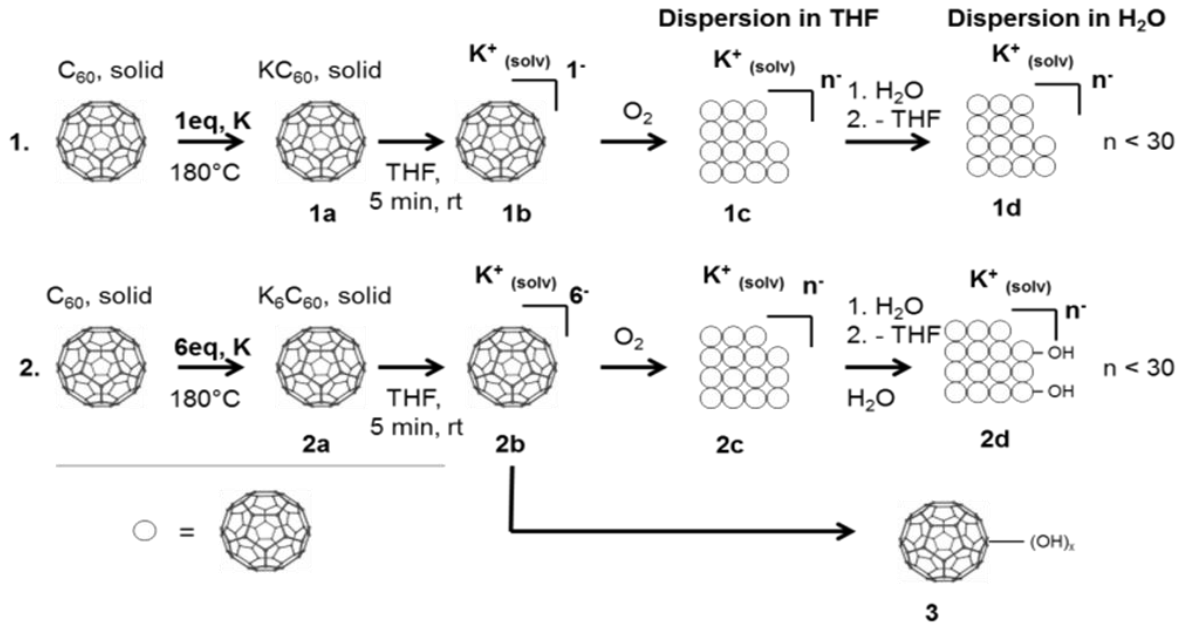

Figure 1. Preparation of aqueous dispersions containing fullerene nanoparticles by two different pathways **1,2** starting from solid C_{60}: (i) Reduction of fullerene by potassium metal; stoichiometry KC_{60} (**1a**) and K_6C_{60} (**2a**); (ii) Dissolution of salts **1a** and **2a** in THF generating fulleride solutions **1b** and **2b**; (iii) Oxidation of the fulleride solutions by air generating the THF dispersions **1c** and **2c**; (iv) Transfer of the THF dispersions to water and formation of the aqueous dispersions **1d** and **2d** after THF evaporation; Fullerenols (**3**) have been isolated from sample **2b** after evaporation of the THF and extracting of the residue by toluene in a Soxhlet extractor followed by column chromatography.

UV-Vis-NIR spectrum of **1b** exhibits bands at 991 and 1074 nm, typical of the C_{60}^{-} anion,[6,16,17,26] and bands at 827 and 985 nm, characteristic of C_{60}^{2-} dianion,[6,17,26] suggesting that a mixture between the two fullerene anions is present in solution (see Figure 2A). UV-Vis-NIR spectrum of **2b** shows a band at 335 nm with low intensity characteristic of fullerene electronic transition, also seen in the spectrum of solution **1b**. According to literature, the electronic states of C_{60} are not too much affected by anion formation,[36] so some electronic transitions of pristine fullerene can also be seen in doped C_{60}.

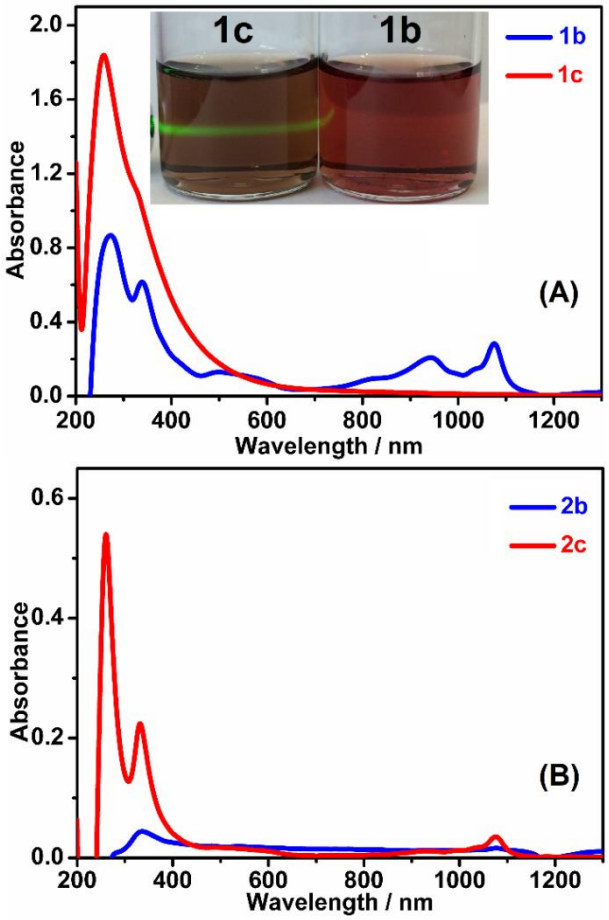

Figure 2. UV-Vis-NIR spectra of samples **1b** and **1c** (A); Inserted: pictures of samples **1c** and **1b** irradiated by green laser; UV-Vis-NIR spectra of samples **2b** and **2c** (B).

Both fulleride solutions were then bubbled with air to promote oxidation and a visible colour change was observed in each case (see Fig. S3). This oxidation step lowers the overall charge density, leading to a destabilization of the solutions and the formation of C_{60} nanoparticles in THF. The change from solution (**1b**) to dispersion (**1c**) can be visualized by the Tyndall effect: the formation of aggregates of size close to the wavelength of an incident radiation provokes scattering (see insert in Figure 2A). This is confirmed by DLS measurements that show particles with mean diameter equal to 200 nm for sample **1c** (see Table S1 in ESI). This behaviour change, from solution to dispersion, does not depend on the

initial electron density as in both cases metastable THF dispersions (**1c**, **2c**) could be generated. Alternatively, if solution **1b**, not oxidized, is added to oxygen-free water, there is no color change and the solutions remains stable as long as protected from air (see Fig. S4 in ESI). Indeed, only oxygen and not water can oxidize C_{60}^- in agreement with reports[17,26,37] on related systems.

The formation of metastable dispersions (**1c**, **2c**) in organic media that are stable for weeks after exposition of fulleride solutions to air has not been reported in the literature to the best of our knowledge, although fullerenes are known to produce dispersions in polar solvents.[3,38–40] This interpretation can be corroborated by UV-Vis-NIR spectra of **1c** and **2c**, as in both cases the characteristic absorption bands between 700 and 1300 nm of the respective anions vanish and the peaks below 400 nm characteristic of neutral C_{60} broaden and increase (see Figure 2A and 2B).

Just after the oxidation step, THF dispersions **1c** and **2c** were added to water in different proportions (1:1, 1:2, 1:4, 1:8, (dispersion:water)) avoiding transferring any suspended or precipitated material, especially in the case of K_6C_{60} that is less soluble in THF. The mixtures were placed in a fume hood and left opened for 2 days to allow THF evaporation and formation of aqueous dispersions **1d** and **2d**. Dispersions **1d** and **2d** are stable at least for several months and they are yellow to red-brown, depending on the concentration and on the precursor salt (see pictures inserted in Figure 3 (A) and (B)). The concentration of the respective sample ranges from 2.7 to 200 mg L^{-1} (in relation to C_{60}, see Table S1 and details in ESI) and agrees with the proportion used in the synthesis. The colloidal nature pointed out by the Tyndall effect shown in Fig. S5 as well as the yellow-brownish colour are in accordance with other reports on C_{60} aqueous dispersions.[19,23] Figure 3 shows UV-Vis spectra of the dispersions **1d** (A) and **2d** (B) and for both sets of

samples, the same spectral profile is observed corroborating the observation that the generated dispersions are similar regardless of the initial charging ratio.

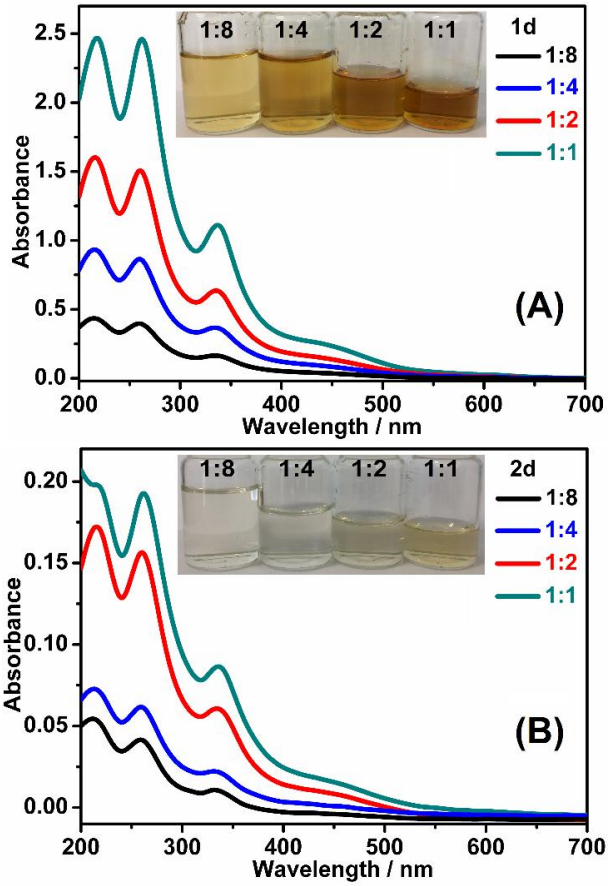

Figure 3. UV-Vis spectra of aqueous dispersions **1d** (A) and **2d** (B) prepared with different concentrations of fulleride solutions and water as indicated inside each graphic. Inset: pictures of aqueous dispersions **1d** in (A) and aqueous dispersions **2d** in (B) prepared with different proportions of fulleride organic dispersions and water.

The overall total absorption is related to the number of dispersed nanoparticles and increases with the ratio between fulleride dispersion and water used. In the corresponding spectra, (Figure 3) absorption bands at 216, 260, and 337 nm can be seen that are linked to electronic transitions of fullerene, present in C_{60} solutions.[3,23] The same bands can be observed in C_{60} saturated solution in THF (see Fig. S6). The broad band between 400 and 500

nm is characteristic of C_{60} dispersions[21,23] and is observed in both set of experiments. These bands are not present in spectra of fullerene solutions (**1b**, **2b**), but are also visible in the THF dispersions (**1c**, **2c**) (see Figure 2) and are responsible for the dispersions color.

In order to understand the chemical nature of those samples, THF dispersions (**1c**, **2c**) have been dried and brown powders have been retained. The solid residues of **1c**, **2c** and C_{60} have been analysed by infrared spectroscopy (IR) (Figure 4). C_{60} has four active IR vibrations,[2] two modes with maxima at 1180 and 1426 cm^{-1}, and the other two next to 530 and 580 cm^{-1} that are not shown. The residue material of **1c** has a similar IR profile to pristine fullerene, except for a band next to 2800 cm^{-1} that may be attributed to C-H stretching vibrations.

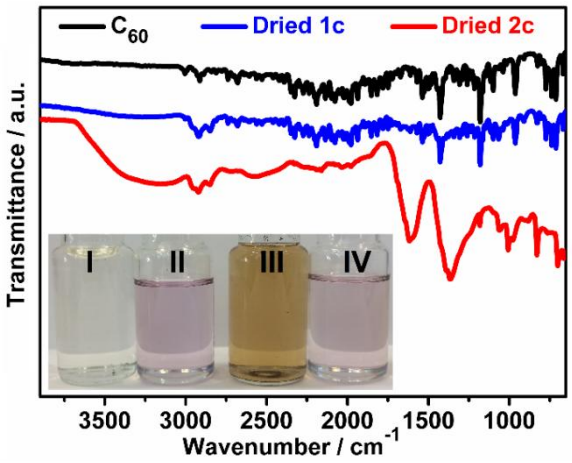

Figure 4. Infrared spectra of pristine C_{60} and dried residues from samples **1c** and **2c**; Inset: pictures of residue from sample **1c** redispersed with water (I) and toluene (II), and residue from sample **2c** redispersed with water (III) and toluene (IV).

Peaks that may be attributed to C-H vibrations are also present in the residue materials of **2c**, at about 2900 cm^{-1}. More importantly, sample **2c** has a distinct profile differing from the other two, with intense and broad absorption bands at 1000, 1363, 1608, and 3150 cm^{-1}, which are attributed to C-OH bending, and C-O, C=O and O-H stretching respectively.[21,41]

This different spectral profile indicates that residue materials of **2c** has a higher content of oxidized fullerene species, fullerenols, than the the residue material of sample **1c**. Elemental analysis showed 88.0 % and 56.7 % of carbon and 5.7 % and 20.1 % of oxygen for the residue materials of **1c** and **2c** respectively, corroborating the IR results for a higher degree of functionalization for sample **2c**.

The residue sample of **1c** and **2c** have been extracted by toluene exhibiting the characteristic purple colour of C_{60} in this solvent[3] for both samples (see insert in Figure 4, II and IV). However, only the residue solid of **2c** and not that of **1c** can be redispersed in water in appreciable extent, as the characteristic brown colour can only be seen in flask (III) and not in flask (I) from Figure 4. This observation corroborates the evidence for surface modification and the higher content of fullerenol for samples with higher initial charging ratios.[3,8,21] Both residue samples of **1c** and **2c** have been dissolved / re-dispersed in deuterated toluene and deuterated water and ^{13}C NMR analysis were performed (see Fig. S7). Consistent with the purple color of the toluene dissolution, ^{13}C NMR spectrum shows the characteristic signal of C_{60} at 143 ppm.

Raman spectra of the residue samples of **1c** and **2c** exhibit a similar spectral profile to pristine fullerene with the A_g mode at 1463 cm^{-1}, suggesting that a significant content of C_{60} is preserved in each case after the oxidation step (see Fig. S8). Interestingly, the presence of fullerenol in the aqueous dispersion is crucial for repeated re-dispersibility from the powder and is only possible for sample **2c**. However, redispersed sample from residue of **2c** is composed by nanoparticles of mean diameter close to 380 nm (see Table S1), suggesting that those fullerenol nanoparticles are formed by a core made mostly of pristine C_{60} and a shell enriched in fullerenols. Thus, a purification has been performed, based on Soxhlet extraction followed by column chromatography (details see Figure 1 and ESI) and a molecular fullerenol sample (**3**) has been extracted. The first fraction contains non-functionalized fullerenes,

indicated by the deep purple colour and analysed by mass spectrometry, UV-Vis, and NMR (see Fig. S9-11). The remaining fractions contain differently functionalized fullerenols, although no symmetric or pure product could be obtained. This observation highlights the complex oxidation process and shows the demand to understand the fundamental reaction steps occurring in more detail.

The molecular reaction mechanism for fullerenols formation is complex as evidenced by the heterogeneity of the sample composition. Similar charged carbon materials (potassium salts of carbon nanotubes), also sensitive towards oxygen and water from atmosphere, have been studied extensively.[31] A similar mechanism is probably occurring for fullerides. Upon discharging of the carbon lattice, the C_{60} molecules start to form nanoparticles, because the electrostatic repulsion is diminished. When oxygen is used as oxidant, single electron transfer is occurring and forming superoxide radical anions.[37] Those can either react with the exposed surface of the nanoparticles, which leads to the generation of fullerenols or they can disproportionate in water, which does not lead to functionalization. Thus, the larger the amount of potassium, the larger the amount of produced fullerenols.

Aqueous dispersions **1d** and **2d** are composed of polydisperse nanoparticles (See Fig. S12) with mean diameters between 25 and 70 nm as measured by DLS (see Table S1). Interestingly, the final size of the particles in aqueous dispersions (**1d**, **2d**) diminishes when the amount of water increases vs that of THF dispersion (**1c**, **2c**). Most of these nanoparticles are formed by pristine C_{60} as shown by IR, Raman and redissolution experiments, with more functional groups in the case of **2d** dispersions. The nanoparticles exhibit zeta potentials from -10 to -50 mV as shown in Table S1, which is higher for aqueous dispersions obtained with higher content of fulleride solutions (1:1). Aqueous dispersions **1d** and **2d** are homogeneous in the whole volume and no aggregation was observed after one year of storage in closed glass flasks.

TEM images for aqueous dispersions (**1d** and **2d**, 1:2 proportion) are shown in Fig. S13 (a,b). In both samples, a size distribution is visible spanning from a few nanometers up to about 60 nm, and a fraction of larger particles coexists with a fraction of smaller particles. The apparent distribution is agreement with the average particle size distribution by DLS, considering that the latter emphasizes larger particles. HR-TEM images for are shown in Fig. S14 (**1d**) and S15 (**2d**). Crystalline nanoparticles can be found in aqueous dispersion **1d** (Fig. S14 a,b), evidenced by the FFT analysis (Fig. S14 c) of the respective particle (Fig. S14 b). Nanoparticles observed for dispersion **2d** are significantly less ordered as evidenced by the FFT analysis (Fig. S15 c) of the respective particle (Fig. S15 b).

Due to the low degree of functionalization and to their non- re-dispersibility after water addition (see Figure 4), dispersions **1d** are lyophobic and the colloidal stability of those is provided by electrostatic repulsion.[19,42–45] So, these dispersions can be considered as model to apply DLVO theory for carbon-based systems,[30] as has been done for fullerene dispersions made by other routes.[3,19,44–46] Figure 5A presents a graphic of total interaction energy (U_T) as a function of distance for two identical spherical particles calculated based on DLVO theory,[47,48] considering the experimental radius (half of the diameters shown in Table S1) and zeta potentials for **1d** dispersions, an approximate value for Hamaker constant ($1^{x}10^{-19}$ J) from literature,[3] and 1:1 electrolyte ($1 \cdot 10^{-1}$ mmol L^{-1}). The kinetic barriers against coagulation increase with concentration for dispersions **1d** because concentrated systems have bigger nanoparticles with higher zeta potentials as shown in Table S1. These zeta potentials provide electrostatic stabilization for aqueous dispersions **1d**. For the most concentrated system, a kinetic barrier higher than $45k_BT$ is achieved, which is enough to keep the system stable for long periods.[47,49]

Dispersions **2d** exhibit a higher contribution of solvation by water due to the presence of fullerenols. Thus, their colloidal behaviour is more complex, and a combination of different

effects is expected. It has been shown that fullerenols with about 15 hydroxyl groups are barely water soluble and only with 36 or more functional groups, water solubility could be reached.[15] The degree of functionalization of dispersions **1d** and **2d** and fullerenol sample **3** is way lower than this threshold value, as evidenced by mass spectroscopy (see Fig. S9), and thus the stabilization of the dispersions is mainly provided by the electrical charges on dispersed nanoparticles evidenced by zeta potential measurements rather than by functional groups. However, the re-dispersibility of the residue sample of **2c** is strongly connected with the presence of functional groups.

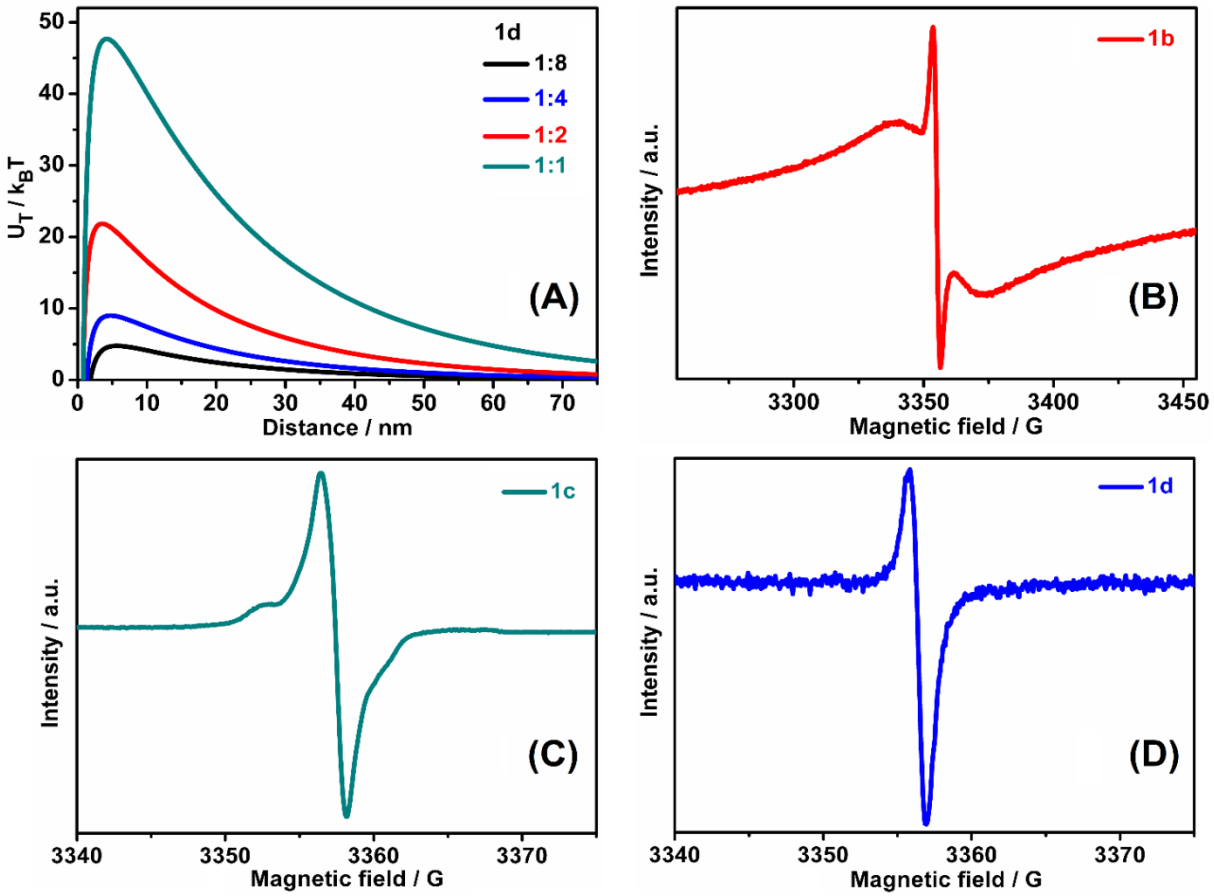

Figure 5. Graphic of total interaction energy in terms of thermal energy in function of distance for two spherical particles according to DLVO theory for **1d** dispersions (A); ESR spectrum of concentrated **1b** solution in THF (B); ESR spectrum of concentrated **1c** dispersion in THF (C); ESR spectrum of concentrated **1d** dispersion in water (D).

Therefore, it is important to identify the origin of the charges in these dispersions leading to negative zeta potentials, especially on low functionalized systems because reports about stable radicals are related with higher content of fullerenols.[8] Thus, Electron Spin Resonance (ESR) measurements where conducted on the samples **1b**, **1c** and **1d** (Figure 5B-D) prepared following the same procedure, but with higher material concentration (five times the concentration of **1b** used before).

ESR spectrum from solution **1b** shown in Figure 5B has a broad signal (ΔH_{pp} = 35 G) at g = 1.9996 ± 0.0003, characteristic of C_{60}^- anion radicals[16,17,37,50] with an integrated intensity of about 1.6^x10^{-9} emu cm^{-3} (8^x10^{17} equivalent S=1/2 Curie spins cm^{-3}). A second and much narrower signal is present at a slightly higher g = 2.0003 ± 0.0003, but with a linewidth $\Delta H_{pp} \sim 3$ G and a relative intensity 100 times smaller. This sharp signal is likely to arise from $C_{120}O^{n-}$ impurities (n odd).[50] After oxidation by air-exposure, the ESR spectra are significantly modified. The spectrum of dispersion **1c** is at g = 2.0020 ± 0.0003, with $\Delta H_{pp} \sim$ 1.8 G and the total intensity is decreased by almost two orders of magnitude down to 3.2^x10^{-11} emu cm^{-3}. The main line is slightly asymmetric due to an unresolved axial powder spectrum lineshape. The small bumps on the wings are characteristic of a badly resolved triplet spectrum with g ~ 2.0023 ± 0.0003 and D ~ 5.8 G. The spectrum of dispersion **1d** was difficult to obtain because of the water transfer, however it is very similar to the spectrum of dispersion **1c** (g = 2.0023 ± 0.0003, ΔH_{pp} ~ 1.2 G, intensity ~2.0^x10^{-11} emu cm^{-3}). Most charges have been lost upon oxidation from **1b** to **1c**, as expected. The remaining sharp signal is not significantly different from the impurities arising from off the shelf C_{60},[50] and should probably be ascribed to those.

4. CONCLUSIONS

The developed protocol for the synthesis of dispersions in THF or water is versatile and concentrations up to 200 mg L^{-1} of fullerene C_{60} in water can be reached. Oxidation of fulleride organic solutions with oxygen leads to fullerene nanoparticles dispersed in THF, due to charge loss of most fullerene molecules. This leads to aggregation into nanostructures, forming a metastable dispersion. This dispersion can be transferred to water in different proportions and after evaporation of the THF, aqueous fullerene dispersions composed by size calibrated nanoparticles are generated. The content of functionalized species, i.e. fullerenols, can be tuned by the amount of initial charges during the reduction and dissolution steps. Those initial charges have a direct influence on the re-dispersibility of the C_{60} dispersions. Samples with a content of fullerenols can be redispersed, while those exhibiting almost no fullerenols cannot. However, it should be pointed out that even barely functionalized dispersions remain stable due to electrostatic repulsion between individual nanoparticles. Colloidal stability has been checked for months, and are still stable after one year, exceeding by far the minimum demand for processability.

ASSOCIATED CONTENT

Supporting information

The Supporting Information has all experimental procedures, samples characterization, some complementary figures, pictures, and table (PDF).

Conflicts of interest

There are no conflicts to declare.

Author Contributions

JPVD and FH have performed all the experiments, sample analysis, interpretation, and discussion of results. OC has performed the ESR experiments. AJGZ and AP have collaborated in the interpretation and discussion of results. All authors have contributed on writing the manuscript.

ACKNOWLEDGMENTS

JPVD acknowledges CAPES for the fellowship and funding to stay in CRPP at Bordeaux, France (CAPES-PrInt). We thank CAPES, CNPq, Fundação Araucária and INCT Nanocarbonos for research funding and CAPES-COFECUB (grant PH-C931/19 - 42002PK) for collaboration grant. FH and AP thank the French ANR (EdgeFiller project). FH thanks CNRS (Momentum grant). We thank Christelle Absalon for the results of mass spectrometry.

REFERENCES

[1] H.W. Kroto, J.R. Heath, S.C. O'Brien, R.F. Curl, R.E. Smalley, C_{60}: Buckminsterfullerene, Nature. 318 (1985) 162–163. doi:10.1038/318162a0.

[2] W. Krätschmer, L.D. Lamb, K. Fostiropoulos, D.R. Huffman, Solid C_{60}: a new form of carbon, Nature. 347 (1990) 354–358. doi:10.1038/347354a0.

[3] N.O. McHedlov-Petrossyan, Fullerenes in liquid media: An unsettling intrusion into the solution chemistry, Chem. Rev. 113 (2013) 5149–5193. doi:10.1021/cr3005026.

[4] N.O. Mchedlov-Petrossyan, Fullerenes in molecular liquids. Solutions in "good" solvents: Another view, J. Mol. Liq. 161 (2011) 1–12. doi:10.1016/j.molliq.2011.04.001.

[5] R.S. Ruoff, D.S. Tse, R. Malhotra, D.C. Lorents, Solubility of fullerene (C_{60}) in a variety of solvents, J. Phys. Chem. 97 (1993) 3379–3383. doi:10.1021/j100115a049.

[6] I. Wabra, J. Holzwarth, F. Hauke, A. Hirsch, Exohedral Addition Chemistry of the Fullerenide Anions C_{60}^{2-} and $C_{60}^{\cdot-}$, Chem. - A Eur. J. 25 (2019) 5186–5201. doi:10.1002/chem.201805777.

[7] F. Machui, S. Langner, X. Zhu, S. Abbott, C.J. Brabec, Determination of the P3HT:PCBM solubility parameters via a binary solvent gradient method: Impact of solubility

on the photovoltaic performance, Sol. Energy Mater. Sol. Cells. 100 (2012) 138–146. doi:10.1016/j.solmat.2012.01.005.

[8] L.O. Husebo, B. Sitharaman, K. Furukawa, T. Kato, L.J. Wilson, Fullerenols revisited as stable radical anions, J. Am. Chem. Soc. 126 (2004) 12055–12064. doi:10.1021/ja047593o.

[9] K. Kokubo, K. Matsubayashi, H. Tategaki, H. Takada, T. Oshima, Facile synthesis of highly water-soluble fullerenes more than half-covered by hydroxyl groups, ACS Nano. 2 (2008) 327–333. doi:10.1021/nn700151z.

[10] J. Wu, L.B. Alemany, W. Li, D. Benoit, J.D. Fortner, Photoenhanced transformation of hydroxylated fullerene (fullerol) by free chlorine in water, Environ. Sci. Nano. 4 (2017) 470–479. doi:10.1039/c6en00381h.

[11] Y.I. Prylutskyy, V.I. Petrenko, O.I. Ivankov, O.A. Kyzyma, L.A. Bulavin, O.O. Litsis, M.P. Evstigneev, V. V. Cherepanov, A.G. Naumovets, U. Ritter, On the origin of C_{60} fullerene solubility in aqueous solution, Langmuir. 30 (2014) 3967–3970. doi:10.1021/la404976k.

[12] C.M. Sayes, J.D. Fortner, W. Guo, D. Lyon, A.M. Boyd, K.D. Ausman, Y.J. Tao, B. Sitharaman, L.J. Wilson, J.B. Hughes, J.L. West, V.L. Colvin, The differential cytotoxicity of water-soluble fullerenes, Nano Lett. 4 (2004) 1881–1887. doi:10.1021/nl0489586.

[13] L.Y. Chiang, J.W. Swirczewski, C.S. Hsu, S.I. Chowdhury, S. Cameron, K. Creegan, Multi-hydroxy Additions onto C_{60} Fullerene Molecules, J. Chem. Soc. Chem. Commun. 24 (1992) 1791–1793. doi:10.1039/C39920001791.

[14] S. Wang, P. He, J.M. Zhang, H. Jiang, S.Z. Zhu, Novel and efficient synthesis of water-soluble [60]fullerenol by solvent-free reaction, Synth. Commun. 35 (2005) 1803–1808. doi:10.1081/SCC-200063958.

[15] K. Kokubo, S. Shirakawa, N. Kobayashi, H. Aoshima, T. Oshima, Facile and scalable synthesis of a highly hydroxylated water-soluble fullerenol as a single nanoparticle, Nano Res. 4 (2011) 204–215. doi:10.1007/s12274-010-0071-z.

[16] C.A. Reed, R.D. Bolskar, Discrete Fulleride Anions and Fullerenium Cations, Chem. Rev. 100 (2000) 1075–1120. doi:10.1021/cr980017o.

[17] M. Wu, X. Wei, L. Qi, Z. Xu, A new method for facile and selective generation of C_{60}^{-} and C_{60}^{2-} in aqueous caustic/THF (or DMSO), Tetrahedron Lett. 37 (1996) 7409–7412. doi:10.1016/0040-4039(96)01613-9.

[18] A.J. Clancy, M.K. Bayazit, S.A. Hodge, N.T. Skipper, C.A. Howard, M.S.P. Shaffer, Charged Carbon Nanomaterials: Redox Chemistries of Fullerenes, Carbon Nanotubes, and Graphenes, Chem. Rev. 118 (2018) 7363–7408. doi:10.1021/acs.chemrev.8b00128.

[19] N.O. Mchedlov-Petrossyan, V.K. Klochkov, G. V. Andrievsky, Colloidal dispersions of fullerene C_{60} in water: Some properties and regularities of coagulation by electrolytes, J. Chem. Soc. Faraday Trans. 93 (1997) 4343–4346. doi:10.1039/a705494g.

[20] G. V. Andrievsky, M. V. Kosevich, O.M. Vovk, V.S. Shelkovsky, L.A. Vashchenko, On the production of an aqueous colloidal solution of fullerenes, J. Chem. Soc. Chem. Commun. (1995) 1281–1282. doi:10.1039/C39950001281.

[21] L. Pospísil, M. Gál, M. Hromadová, J. Bulícková, V. Kolivoska, J. Cvacka, K. Nováková, L. Kavan, M. Zukalová, L. Dunsch, Search for the form of fullerene C_{60} in aqueous medium, Phys. Chem. Chem. Phys. 12 (2010) 14095–14101. doi:10.1039/c0cp00986e.

[22] A. Dhawan, J.S. Taurozzi, A.K. Pandey, W. Shan, S.M. Miller, S.A. Hashsham, V. V. Tarabara, Stable colloidal dispersions of C_{60} fullerenes in water: Evidence for genotoxicity, Environ. Sci. Technol. 40 (2006) 7394–7401. doi:10.1021/es0609708.

[23] S. Deguchi, R.G. Alargova, K. Tsujii, Stable Dispersions of Fullerenes, C_{60} and C_{70}, in Water. Preparation and Characterization, Langmuir. 17 (2001) 6013–6017. doi:10.1021/la010651o.

[24] M.E. Hilburn, B.S. Murdianti, R.D. Maples, J.S. Williams, J.T. Damron, S.I. Kuriyavar, K.D. Ausman, Synthesizing aqueous fullerene colloidal suspensions by new solvent-exchange methods, Colloids Surfaces A Physicochem. Eng. Asp. 401 (2012) 48–53. doi:10.1016/j.colsurfa.2012.03.010.

[25] S. Andreev, D. Purgina, E. Bashkatova, A. Garshev, A. Maerle, I. Andreev, N. Osipova, N. Shershakova, M. Khaitov, Study of Fullerene Aqueous Dispersion Prepared by Novel Dialysis Method: Simple Way to Fullerene Aqueous Solution, Fullerenes, Nanotub. Carbon Nanostructures. 23 (2015) 792–800. doi:10.1080/1536383X.2014.998758.

[26] X. Wei, M. Wu, L. Qi, Z. Xu, Selective solution-phase generation and oxidation reaction of C_{60}^{n-} (n = 1,2) and formation of an aqueous colloidal solution of C_{60}, J. Chem. Soc. Perkin Trans. 2. (1997) 1389–1394. doi:10.1039/a607336k.

[27] G. Bepete, E. Anglaret, L. Ortolani, V. Morandi, K. Huang, A. Pénicaud, C. Drummond, Surfactant-free single-layer graphene in water, Nat. Chem. 9 (2017) 347–352. doi:10.1038/nchem.2669.

[28] G. Bepete, F. Hof, K. Huang, K. Kampioti, E. Anglaret, C. Drummond, A. Pénicaud, ”Eau de graphene” from a KC_8 graphite intercalation compound prepared by a simple mixing of graphite and molten potassium, Phys. Status Solidi RRL. 10 (2016) 895–899. doi:10.1002/pssr.201600167.

[29] G. Bepete, N. Izard, F. Torres-Canas, A. Derré, A. Sbardelotto, E. Anglaret, A. Pénicaud, C. Drummond, Hydroxyl Ions Stabilize Open Carbon Nanotubes in Degassed Water, ACS Nano. 12 (2018) 8606–8615. doi:10.1021/acsnano.8b04341.

[30] J.P. V. Damasceno, A.J.G. Zarbin, A new approach for the achievement of stable aqueous dispersions of carbon nanotubes, Chem. Commun. 55 (2019) 5809–5812. doi:10.1039/c9cc01541h.

[31] F. Hof, S. Bosch, S. Eigler, F. Hauke, A. Hirsch, New basic insight into reductive functionalization sequences of single walled carbon nanotubes (SWCNTs), J. Am. Chem. Soc. 135 (2013) 18385–18395. doi:10.1021/ja4063713.

[32] M.S. Dresselhaus, G. Dresselhaus, P.C. Eklund, Raman Scattering in Fullerenes, J. Raman Spectrosc. 27 (1996) 351–371. doi:10.1002/(SICI)1097-4555(199603)27:3/4<351::AID-JRS969>3.0.CO;2-N

[33] H. Kuzmany, M. Matus, B. Burger, J. Winter, Raman Scattering in C_{60} fullerenes and fullerides, Adv. Mater. 6 (1994) 731–745. doi:10.1002/adma.19940061004.

[34] D.M. Poirier, J.H. Weaver, KC_{60} fulleride phase formation: An x-ray photoemission study, Phys. Rev. B. 47 (1993) 10959. doi:10.1103/PhysRevB.47.10959.

[35] S.C. Erwin, M.R. Pederson, Electronic structure of crystalline K_6C_{60}, Phys. Rev. Lett. 67 (1991) 1610. doi:10.1103/PhysRevLett.67.1610.

[36] M.S. Dresselhaus, G. Dresselhaus, A.M. Rao, P.C. Eklund, Optical properties of C_{60} and related materials, Synth. Met. 78 (1996) 313–325. doi:10.1016/0379-6779(96)80155-X.

[37] J. Stinchcombe, A. Pénicaud, P. Bhyrappa, P.D.W. Boyd, C.A. Reed, Buckminsterfulleride(1-) Salts: Synthesis, EPR, and the Jahn-Teller Distortion of C_{60}^-, J. Am. Chem. Soc. 115 (1993) 5212–5217. doi:10.1021/ja00065a037.

[38] R.G. Alargova, S. Deguchi, K. Tsujii, Stable colloidal dispersions of fullerenes in polar organic solvents, J. Am. Chem. Soc. 123 (2001) 10460–10467. doi:10.1021/ja010202a.

[39] N.O. Mchedlov-Petrossyan, N.N. Kamneva, Y.T.M. Al-Shuuchi, A.I. Marynin, S.V. Shekhovtsov, The peculiar behavior of fullerene C_{60} in mixtures of 'good' and polar solvents: Colloidal particles in the toluene-methanol mixtures and some other systems, Colloids Surfaces A Physicochem. Eng. Asp. 509 (2016) 631–637. doi:10.1016/j.colsurfa.2016.09.045.

[40] S. Deguchi, S.A. Mukai, Top-down preparation of dispersions of C_{60} nanoparticles in organic solvents, Chem. Lett. 35 (2006) 396–397. doi:10.1246/cl.2006.396.

[41] J. Wu, D.G. Goodwin, K. Peter, D. Benoit, W. Li, D.H. Fairbrother, J.D. Fortner, Photo-Oxidation of Hydrogenated Fullerene (Fullerane) in Water, Environ. Sci. Technol. Lett. 1 (2014) 490–494. doi:10.1021/ez5003055.

[42] J.P.V. Damasceno, A.J.G. Zarbin, Electrostatic stabilization of multi-walled carbon nanotubes dispersed in nonaqueous media, J. Colloid Interface Sci. 529 (2018) 187–196. doi:10.1016/j.jcis.2018.06.002.

[43] A.N.J. Rodgers, M. Velický, R.A.W. Dryfe, Electrostatic Stabilization of Graphene in Organic Dispersions, Langmuir. 31 (2015) 13068–13076. doi:10.1021/acs.langmuir.5b04219.

[44] N.O. Mchedlov-Petrossyan, N.N. Kamneva, Y.T.M. Al-Shuuchi, A.I. Marynin, Interaction of C_{60} aggregates with electrolytes in acetonitrile, Colloids Surfaces A Physicochem. Eng. Asp. 516 (2017) 345–353. doi:10.1016/j.colsurfa.2016.12.035.

[45] N.O. Mchedlov-Petrossyan, N.N. Kamneva, Y.T.M. Al-Shuuchi, A.I. Marynin, O.S. Zozulia, A.P. Kryshtal, V.K. Klochkov, S. V. Shekhovtsov, Towards better understanding of C_{60} organosols, Phys. Chem. Chem. Phys. 18 (2016) 2517–2526. doi:10.1039/C5CP06806A.

[46] N.O. Mchedlov-Petrossyan, N.N. Kamneva, Y.T.M. Al-Shuuchi, A.I. Marynin, O.S. Zozulia, Formation and ageing of the fullerene C_{60} colloids in polar organic solvents, J. Mol. Liq. 235 (2017) 98–103. doi:10.1016/j.molliq.2016.10.113.

[47] D.J. Shaw, Introduction to Colloid and Surface Chemistry, 4th ed., Butterworth-Heinemann, Oxford, UK, (1992).

[48] R.J. Hunter, Foundations of Colloid Science, 2nd ed., Oxford University Press, New York, USA, (2001).

[49] J.T.. Overbeek, Recent developments in the understanding of colloid stability, J. Colloid Interface Sci. 58 (1977) 408–422. doi:10.1016/0021-9797(77)90151-5.

[50] P. Paul, K.-C. Kim, D. Sun, P.D.W. Boyd, C.A. Reed, Artifacts in the electron paramagnetic resonance spectra of C_{60} fullerene ions: Inevitable $C_{120}O$ impurity, J. Am. Chem. Soc. 124 (2002) 4394–4401. doi:10.1021/ja011832f.